



# Large scale fused-granular-fabrication using recycled carbon fibre/PEKK-PEEK pellets derived from aerospace prepreg waste

Ruan-Isabelle Richard Soucy <sup>a</sup>, Adam W. Smith <sup>a</sup>, Kevin Dupuis <sup>c</sup>, Ilyass Tabiai <sup>a,b</sup>, Martine Dubé <sup>a,b,\*</sup> 

<sup>a</sup> Mechanical Engineering Department, École de Technologie Supérieure, Montréal, Canada

<sup>b</sup> Research Center for High Performance Polymer and Composite Systems (CREPEC), Montréal, Canada

<sup>c</sup> Syensqo (previously Part of Solvay Group), Bruxelles, Belgium



## ARTICLE INFO

### Keywords:

Thermoplastic composites  
Recycling  
Additive manufacturing

## ABSTRACT

The manufacturing of thermoplastic unidirectional prepreg rolls involves trimming the edges as they do not meet specifications in terms of thickness and fibre content. This production waste, referred to as tape edge trim (TET), is recycled and transformed into pellets to be used as a feedstock for fused-granular-fabrication (FGF). In the transformation of the TET waste into pellets, neat PEEK polymer is added to the CF/PEKK TET to reduce the fibre content and improve the printability of the material. A large scale six-axis FGF printing robot is employed to print boxes from the recycled and virgin pellets. DSC analyses performed on recycled and virgin pellets reveal the degradation of PEEK and PEKK following aging at 380 °C or 400 °C under oxidative conditions, due to cross-linking reactions. However, no degradation is observed for specimens manufactured by FGF. As commonly observed for parts manufactured using extrusion-based techniques, the standard tensile and flexural specimens extracted from the FGF boxes demonstrate anisotropic mechanical properties. Additional boxes are manufactured by FGF using pellets obtained from shredded FGF box fragments to assess the capability of recycling the material a second time. A reduction of the stiffness and strength of the material is shown for this second recycling, which is assumed to be due to polymer chain scission and reduction in fibre length occurring during the shredding of the printed parts.

## 1. Introduction

### 1.1. Thermoplastic composite production waste

The production of high-performance thermoplastic composite parts generates waste at various stages of the manufacturing cycle, from manufacturing the pre-impregnated material to cutting blanks from pre-consolidated laminates, trimming finished components, and rejecting defective parts. At the beginning of the cycle, the production of the pre-impregnated materials often generates waste known as tape edge trim (TET). This waste comes from the trimming of prepreg edges where non-uniform resin impregnation results in unacceptable variations in fibre volume content or tape thickness. TET waste is typically chopped into pieces, collected and disposed of through landfilling or pyrolysis.

The collected TET waste resembles a form of thermoplastic composite referred to in the literature as “randomly-oriented strands” (ROS) except that their size and shape vary greatly. Despite variations in fibre

content and tape thickness, TET waste remains valuable, often consisting of carbon fibre and high-performance engineering polymers such as poly-ether-ether-ketone (PEEK) or poly-ether-ketone-ketone (PEKK). The authors have previously shown the potential of TET waste to be used in the compression moulding process with the possibility of reducing the material heterogeneity through mechanical sieving [1,2]. Although the TET waste discontinuous reinforcement allows for complex shapes to be manufactured by compression moulding, other processes could offer additional manufacturing freedom. The fused-granular-fabrication (FGF) additive manufacturing (AM) technique is one such process. In order to find new applications for the TET waste, Syensqo has developed an in-house proprietary method that converts TET waste into pellets suitable for use as feedstock in FGF. The recycled pellets studied here consist of CF/PEKK TET with added neat PEEK polymer.

A key focus of this work is to examine the potential degradation of these pellets when printed at temperatures ranging from 380 °C to 400 °C. Previous studies have shown that PEEK and other polymers from

\* Corresponding author. Mechanical Engineering Department, École de Technologie Supérieure, Montréal, Canada.

E-mail address: [martine.dube@etsmtl.ca](mailto:martine.dube@etsmtl.ca) (M. Dubé).

the same family undergo degradation in the form of chain scission or crosslinking when processed at these temperatures in the presence of oxygen. Therefore, this study first investigates the degradation behaviour of the recycled pellets and then evaluates the feasibility of using the FGF process to make parts from them.

### 1.2. Degradation mechanisms and crystallization kinetics

The degradation mechanisms of PEEK and other polymers of the same family often involve chain scission or crosslinking [3–9]. These two mechanisms are known to occur when PEEK is in its molten state, particularly if it is exposed to an oxidative environment. Chain scission decreases the molecular weight and viscosity of the polymer, while crosslinking has the opposite effect. De Almeida [10] has shown the dominant effect of crosslinking over chain scission with a substantial increase in viscosity, measured using a parallel plate rheometer, for PEEK samples subjected to temperatures ranging from 360 °C to 420 °C. Viscosity is a critical factor for the quality of parts produced through FGF, as it directly affects the formation of voids and other defects. Conversely, excessively low viscosity may cause over-extrusion, thereby compromising the geometric accuracy of the final parts.

Crosslinking occurring in PEEK and similar polymers when exposed to oxygen in their molten state also affects the crystallization kinetics and final crystallinity of the material. The crystallinity of the polymer decreases as a result of restricted chain mobility induced by crosslinking reactions. As degradation can significantly impact key properties such as melt viscosity and final crystallinity of PEEK, this study examines the potential degradation that may occur during the FGF process, particularly due to exposure to oxygen while the polymer is in its molten state.

### 1.3. Fused-granular-fabrication of PEEK and PEKK

FGF is also termed as fused pellet manufacturing or modelling (FPM), pellet additive manufacturing (PAM) or screw extrusion additive manufacturing (SEAM). This extrusion-based additive manufacturing technique (Fig. 1) involves layer-by-layer deposition of molten material onto a print bed.

It operates similarly to fused-filament-fabrication (FFF) but uses pellets instead of filament as feedstock. FGF allows a higher material extrusion flow than FFF, making it particularly advantageous for the manufacturing of large-scale parts (e.g., tooling applications). To the best of the authors' knowledge, the literature regarding AM of PEKK is limited, whereas studies on PEEK are more prevalent and focused on small-scale FFF. FGF of PEEK has been shown in previous research, but no studies have incorporated a robotic arm for large-scale

manufacturing. For example, prints are conducted using conventional 3D printers equipped with a custom screw-extruder and 1 mm nozzle, or use CF/PEEK filament with a fibre content of only 5 % [11–13]. It also appears that the literature does not thoroughly address the potential degradation phenomena during FGF processing, despite the observations made in prior studies focused on the aging of PEEK.

It is recognized that the mechanical performance of AM parts is generally inferior to that of parts manufactured through other more traditional processes, such as injection-moulding. In this context, the recycling route for prepreg TET waste using FGF may be a promising solution for applications such as tooling and prototyping, which do not require high mechanical performance.

### 1.4. Objectives

The objective of this study is to evaluate the potential of the FGF process for producing parts from recycled CF/PEKK-PEEK pellets. To achieve this, the potential degradation phenomena occurring in the recycled or virgin pellets is firstly investigated. Following this, parts are printed using the FGF method and characterized through tensile and flexural mechanical testing. The printed parts are then shredded in an attempt to recreate a precursor similar to the initial CF/PEKK-PEEK pellet. The degradation of the material after one and two printing cycles is analyzed and a comparison of mechanical properties with those of injection-moulded and compression-moulded parts is presented.

## 2. Methodology

### 2.1. Materials

This study concerns recycled pellets manufactured by Syensqo derived from CF/PEKK prepreg TET waste. In the process of manufacturing the recycled pellets, neat PEEK polymer is added to reduce the fibre content and improve the material's processability. The final composition of the pellets is 30 %wt CF, 16 %wt PEKK and 54 %wt PEEK. Fig. 2 shows a representative sample of the recycled pellets. KetaSpire® KT-880 CF/PEEK virgin pellets manufactured and commercialized by Syensqo for injection moulding applications are used as a benchmark material. The virgin pellets comprise 30 %wt CF and 70 %wt PEEK polymer.

### 2.2. Thermal stability

The degradation temperature ( $T_d$ ) of recycled and virgin materials is determined by thermogravimetric analysis using a Diamond Pyris TGA from PerkinElmer. The samples are heated in platinum pans from 25 °C to 900 °C at a heating rate of 10 °C/min under controlled oxidizing (air) and inert ( $N_2$ ) environments. The gas flow is 100 mL/min.

To investigate the potential degradation of recycled and virgin materials at FGF processing temperatures (380 °C and 400 °C), differential scanning calorimetry (DSC) (2500 from TA Instruments) tests are

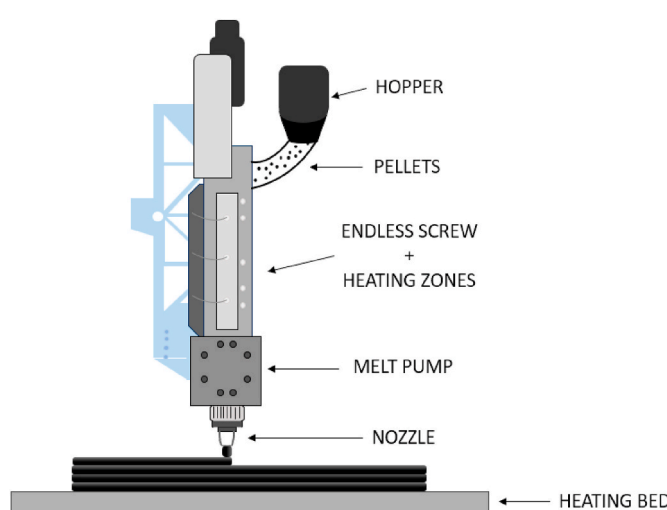


Fig. 1. Schematic of the FGF process.



Fig. 2. CF/PEKK-PEEK recycled pellets made from CF/PEKK pre-impregnated tape edge trims.

conducted. Specimens first undergo a DSC heating/cooling cycle from  $T_1 = 25^\circ\text{C}$  to  $T_2 = 380^\circ\text{C}$  and back to  $T_1 = 25^\circ\text{C}$  at a rate of  $10^\circ\text{C}/\text{min}$  as a baseline. This baseline cycle serves to identify the material's glass transition ( $T_g$ ), melting ( $T_m$ ) and crystallization ( $T_c$ ) temperatures. Subsequently, the samples are transferred to a TGA where they are rapidly heated in air to a temperature  $T_3$  ( $380^\circ\text{C}$  or  $400^\circ\text{C}$ ) for aging. The temperature is maintained for a few minutes (see Table 1) before the samples are cooled back to  $T_1 = 25^\circ\text{C}$ . The samples are then, once again, subjected to the baseline DSC cycle to evaluate potential degradation through a shift in the crystallization peak. This methodology is repeated twice with isothermal dwells in the TGA corresponding to those indicated in Table 1. Aging in an oxidative environment is always performed using TGA, as the DSC equipment cannot operate under oxidative conditions. Other samples undergo the same methodology but are aged in  $\text{N}_2$  environment instead of air. In those cases, the samples are aged directly in the DSC without having to be transferred to a TGA between the DSC cycles. Fig. 3 and Table 1 illustrate and detail the experimental plan. It should be noted that the variability in dwell times is explained by the differences between the given instruction and the real duration due to instrument control.

Finally, samples extracted from FGF printed boxes (see section 2.3) are subjected to a single DSC heating and cooling cycle from  $25^\circ\text{C}$  to  $380^\circ\text{C}$  at a rate of  $10^\circ\text{C}/\text{min}$  to verify if potential degradation occurred during printing.

### 2.3. FGF using recycled CF/PEKK-PEEK pellets or virgin CF/PEEK pellets

The large-scale FGF manufacturing is done using a CEAD AM Flexbot E25 extruder. It consists in a six-axis robot with a  $2.0\text{ m} \times 1.0\text{ m}$  printing bed. The extruder head and the bed can reach a temperature of  $400^\circ\text{C}$  and  $100^\circ\text{C}$ , respectively. During the extrusion process, pellets are heated through five heating zones in the extruder head (Fig. 4). The molten polymer is propelled by the gear pump regulating the flow before the extrusion through a nozzle whose diameter can vary from 2 to 18 mm.

Boxes measuring  $200\text{ mm} \times 200\text{ mm} \times 200\text{ mm}$  are printed at two different temperatures. The heating zone temperatures from zone 1 to 5 are the following:  $360/365/370/375/380^\circ\text{C}$  for boxes noted as RP1, RP2, VP1 and VP2, and  $360/370/380/390/400^\circ\text{C}$  for boxes noted as RP3, RP4, VP3 and VP4. The number of boxes produced is dictated by the amount of pellets available from the manufacturer. The complete processing conditions are reported in Table 2. The layer time refers to the time required to complete the material deposition of a single layer. An example of the boxes manufactured by the FGF process is illustrated in Fig. 4. As specified, the  $X$  axis follows the printing direction and the  $Z$  axis follows the layer stacking direction.

The FGF boxes are subsequently cut into four plates and symmetrically machined to achieve a final thickness of  $3.2 \pm 0.4\text{ mm}$ . This machining process effectively eliminates surface roughness caused by the printing beads as it affects significantly the mechanical properties due to induced stress concentration [15]. Tensile and flexural test specimens are obtained from the plates. Samples are also extracted from the boxes for DSC testing to verify potential degradation during

**Table 1**

Isothermal dwells (1, 2 and 3 on Fig. 3) for tests conducted at  $380^\circ\text{C}$  and  $400^\circ\text{C}$  in air and  $\text{N}_2$ .

Temperature	Environment	Isothermal dwell (mins)					
		Recycled CF/PEKK-PEEK pellet			Virgin CF/PEEK pellet		
		1	2	3	1	2	3
$T_3 = 380^\circ\text{C}$	Air (TGA)	7	17	27	8	18	28
	$\text{N}_2$ (DSC)	10	20	30	10	20	30
$T_3 = 400^\circ\text{C}$	Air (TGA)	8	18	28	8	18	28
	$\text{N}_2$ (DSC)	10	20	30	10	20	30

fabrication by FGF as mentioned in the previous section.

### 2.4. Mechanical testing

Samples extracted from the printed boxes are subjected to mechanical tensile and flexural tests using an MTS Alliance RF/200 machine. Samples are prepared in two orientations for both tests:  $0^\circ$ – aligned with the printing filament axis ( $X$  axis), and  $90^\circ$ – perpendicular to the filament orientation ( $Z$  axis). Samples extracted from compression-moulded panels made of recycled CF/PEKK-PEEK pellets or virgin CF/PEEK pellets (see section 2.7) are also mechanically tested to compare against FGF samples. According to the ASTM D638 standard for tensile testing, Type I specimens are clamped between mechanical self-tightening wedges and tested in displacement-controlled mode at a speed of  $5\text{ mm/min}$ , with strain recorded using an MTS 634.25E-25 extensometer. Three-point bending tests are done following the ASTM D790 standard with a  $1\text{ kN}$  load cell and a  $51\text{ mm}$  support span. Flexural specimens' dimensions are  $127\text{ mm} \times 12.7\text{ mm} \times 3.2\text{ mm}$ . The testing speed is  $1.37\text{ mm/min}$ , corresponding to a strain rate of  $0.01\text{ mm/mm/min}$ . Seven to 15 samples are tested for each configuration for a total of 268 mechanical tests. The mechanical performance of FGF specimens is compared to that of injection-moulded specimens made of virgin and recycled pellets. The injection moulding processing parameters are given in Table 3. Following the mechanical tests, the fractured surfaces are examined using a scanning electron microscope (Hitachi TM3000).

### 2.5. Shredding and second recycling

The printed boxes are shredded using an industrial RS30-450-22 shredder from UNTHA (Fig. 5-a) fitted with a  $15\text{ mm}$  screen, with the aim of recycling the material for another printing cycle. Fig. 5-b shows a representative picture of the shredded material. Direct reuse of shredded chips proved inconclusive in Mortier [16]. The fragment's sharp angles, rough surface finish, and inconsistent size, caused clogging in the transport tube and hopper. Consequently, another step to pelletize the material is necessary to enable successful material reuse in the extruder. The fragments are then shredded again with a Cumberland 6508 device and a  $3/16\text{ in}$  screen prior to pelletization at  $380^\circ\text{C}$  with a single-screw Brabender 203-5HP extruder. The pellets obtained are shown in Fig. 5-c. They are used in another printing cycle using the same parameters as described in Table 2 of section 2.3, with an extrusion temperature of  $380^\circ\text{C}$  for heat zone 5. The printed boxes made of this twice recycled material are cut and machined, and samples are extracted for mechanical testing as detailed in section 2.4.

### 2.6. Micro computed tomography

Micro computed tomography (micro-CT) generates cross-sectional images of an object by measuring the attenuation of X-rays. These 2D projection images are then reconstructed using algorithms to allow 3D representation of the internal structure. Micro-CT is conducted using a ZEISS Xradia 520 X-ray microscope to determine the carbon fibre length in the PEKK-PEEK matrix. Samples and scanning parameters are given in Table 4. The voxel size corresponds to  $1.25\text{ }\mu\text{m}$  and 3201 projections are acquired for each specimen.

The scanning voltage and power are reduced for the fragment samples to enhance contrast. The data is processed using the *Open Fiber Segmentation* tool in *DragonFly* software to determine the fibre length. Approximately 57,000 to 60,000 fibres are measured for the as-received pellets and for the fragments obtained from shredded FGF boxes, while approximately 38,000 fibres are analyzed for the twice-recycled pellets.

### 2.7. Compression moulding

Panels are manufactured via compression moulding using a 70 tons hot press, from which tensile and flexural specimens are extracted to

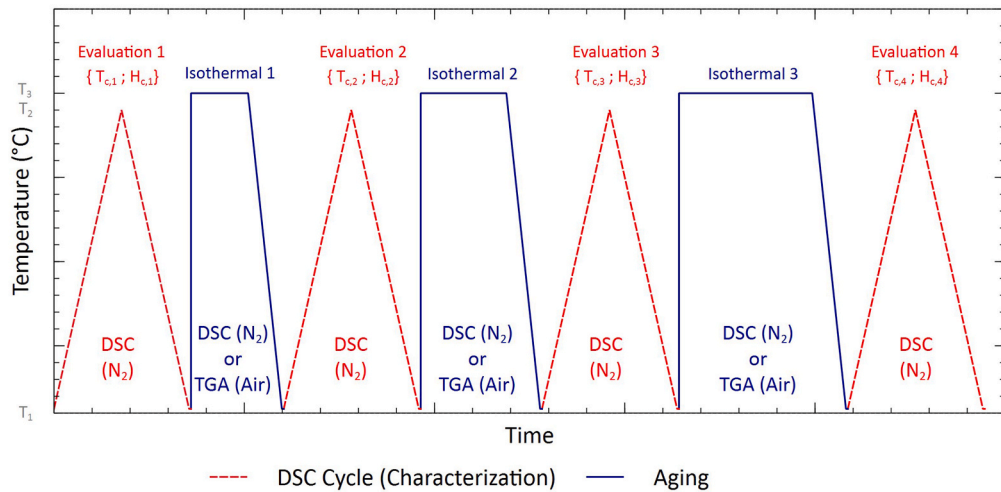


Fig. 3. Test procedure tailored for an investigation into possible degradation in air and  $N_2$ .

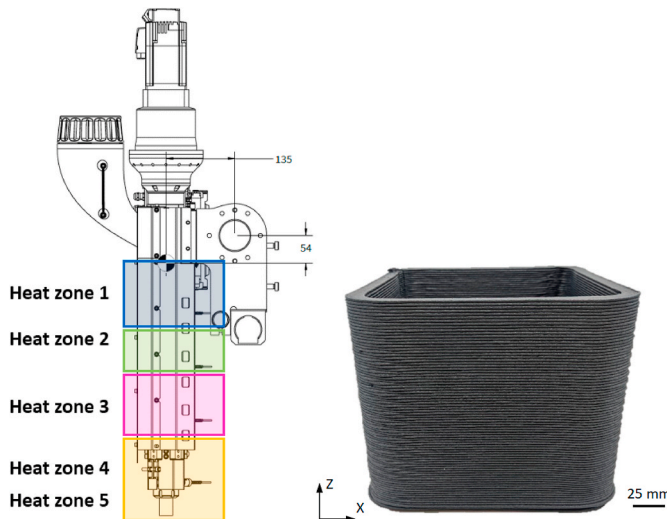


Fig. 4. Schematic of the five heating zones (adapted from CEAD documentation [14]) and a test box manufactured by FGF using CF/PEKK-PEEK recycled pellets.

Table 2  
FGF CEAD AM Flexbot E25 processing conditions.

Material	Box RP1 to RP4: Recycled CF/PEKK-PEEK pellets Box VP1 to VP4: Virgin CF/PEEK pellets
Pellets drying temperature/Time prior to printing	120 °C/5 h
Extrusion temperature (Heat zone 5)	Boxes RP1, RP2, VP1 and VP2: 380 °C Boxes RP3, RP4, VP3 and VP4: 400 °C
Nozzle diameter	9 mm (flat)
Layer height	2.5 mm
Layer time	30 s

enable a comparative analysis of mechanical performance with FGF samples. Pellets are introduced in the mould cavity to manufacture plates measuring 305 mm  $\times$  305 mm  $\times$  3.2 mm. Three thermocouples are placed at different locations within the mould (middle, corner and edge) to monitor temperature variations during the consolidation cycle. The platens are heated to 385 °C at a rate of 10 °C/min under an applied pressure of 0.75 MPa. Once the processing temperature is reached, the pressure is increased to 1.0 MPa for a dwell of 30 min. This pressure is

Table 3  
Injection-moulding parameters (from Syensqo datasheet).

Parameter	Units	Value
Mould temperature	°C	177–204
Rear zone temperature	°C	365
Middle zone temperature	°C	371
Front zone temperature	°C	377
Nozzle temperature	°C	382
Injection speed	cm/sec	2.5–7.5 (Moderate)
Injection pressure	MPa	24
Back pressure	MPa	2
Screw speed	rpm	75–100
Screw compression ratio	–	2.5:1.0 to 3.5:1.0

maintained during cooling at a rate of 10 °C/min until the temperature approaches 100 °C, at which point the panel is demoulded. A representative panel is illustrated in Fig. 6. A total of four panels are manufactured, two made of recycled CF/PEKK-PEEK pellets and two made of virgin CF/PEEK pellets. Samples are extracted from the panels for mechanical testing as explained in section 2.4.

### 3. Results & discussion

#### 3.1. Thermal stability

The degradation temperatures obtained by TGA for the recycled CF/PEKK-PEEK pellets are compared to those of the virgin CF/PEEK pellets and to the values from the literature (Table 5). The reported temperatures are calculated for a 5 % mass loss in order to compare with the values from Zhang [17].

The degradation temperatures in air for both recycled and virgin pellets are lower than those obtained in  $N_2$  which is consistent with findings from the literature. The experimental values are close to the range given by the literature.

Transition temperatures obtained by DSC are given in Table 6. They are taken from the DSC baseline scan, i.e., the first heating and cooling cycle (Evaluation 1) before aging, as explained in the methodology (see Section 2.2). The values sourced from the datasheet of KetaSpire KT-880 virgin pellets are also presented for comparison.

The subsequent thermograms present the DSC heating and cooling curves of samples that underwent the cycles detailed in Section 2.2.

Fig. 7 presents the heating and cooling curves of a recycled CF/PEKK-PEEK pellet that underwent the cycle shown in Fig. 3 with aging at 380 °C in air. A decrease in the melting temperature (from 342 °C to 333 °C) and a 17 % decrease in the enthalpy of fusion after 51 min of

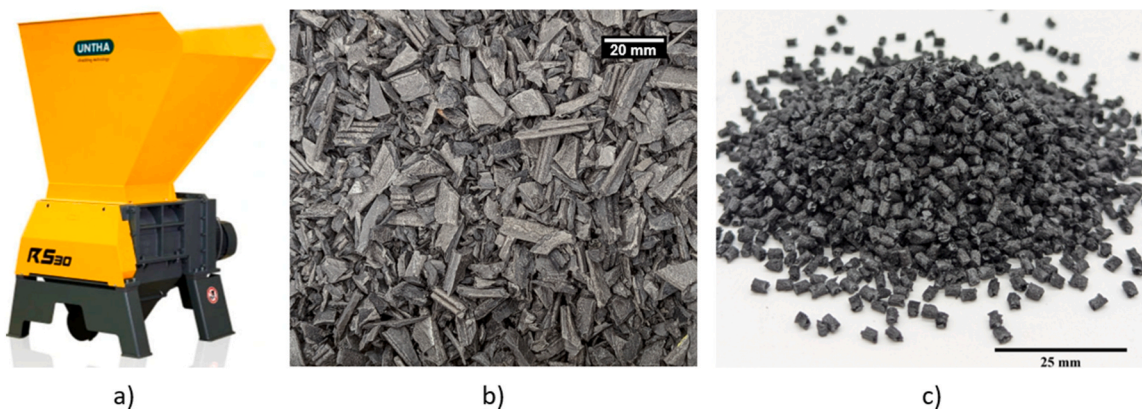


**Fig. 5.** (a) Industrial shredder (from UNTHA shredding technology documentation, 2020), (b) Representative fragments from shredded FGF boxes, (c) CF/PEKK-PEEK pellets obtained from shredded FGF boxes fragments (2nd recycling).

**Table 4**  
Micro computed tomography scanning parameters.

Sample	Voltage (kV)	Power (W)
As-received CF/PEKK-PEEK recycled pellets (Fig. 2)	50	4
Fragments from shredded FGF boxes (1st shredding) (Fig. 5b)	40	3
Recycled pellets obtained after second shredding + pelletization (2nd recycling) (Fig. 5c)	50	4

aging at 380 °C in air is noted. In addition, degradation of PEEK and PEKK is assumed to take place and to intensify with longer exposure to air as a significant shift of 30 °C in the crystallization temperature and a decrease of 17 % in the enthalpy of crystallization are obtained after the sample has completed the full aging cycle, relative to the baseline. These observations align with previous studies on PEEK [3,4], which claim that degradation occurs at low temperatures in air in the form of crosslinking reactions, resulting in a reduction in crystallinity.

Fig. 8 illustrates the thermogram of a virgin CF/PEEK pellet after undergoing the same cycle as the recycled CF/PEKK-PEEK pellet presented in Fig. 7. The degradation is also indicated by the shift in the crystallization temperature and the decrease in the crystallization enthalpy as the peaks become progressively wider. However, the crystallization behaviour of the virgin pellets differs from that of the recycled pellets as the thermogram shows seemingly two crystallization peaks after aging, suggesting the presence of distinct crystalline structures. These two peaks only appear after aging of the CF/PEEK pellets,

**Table 5**

Experimental degradation temperatures in air and N<sub>2</sub>. Comparison between the recycled CF/PEKK-PEEK pellets, virgin CF/PEEK pellets and literature findings [17].

Material	TGA in Air		TGA in N <sub>2</sub>	
	T <sub>d</sub> (°C) <sup>a</sup>			
Recycled Pellets (CF/PEKK-PEEK)	568		576	
Virgin Pellets (CF/PEEK)	570		579	
Neat PEEK [17]	567		582	
CF30-PEEK [17]	561		573	

<sup>a</sup> Corresponding to a mass loss of 5 %.

**Table 6**

Comparison between thermal transition temperatures obtained by DSC for the recycled CF/PEKK-PEEK pellets, virgin CF/PEEK pellets and values from the manufacturer datasheet for virgin pellets.

Transition	Recycled Pellets (CF/PEKK-PEEK)	Virgin Pellets (CF/PEEK)	Virgin Pellets <sup>b</sup> (CF/PEEK)
T <sub>g</sub>	142.4 ± 0.8 °C	149.2 ± 0.4 °C	147 °C <sup>b</sup>
T <sub>m</sub>	344.0 ± 0.4 °C	345.0 ± 0.5 °C	343 °C <sup>b</sup>
T <sub>c</sub>	293.3 ± 0.5 °C	299.4 ± 0.6 °C	n/a

<sup>a</sup> From Syensqo datasheet.

<sup>b</sup> ASTM D3418.

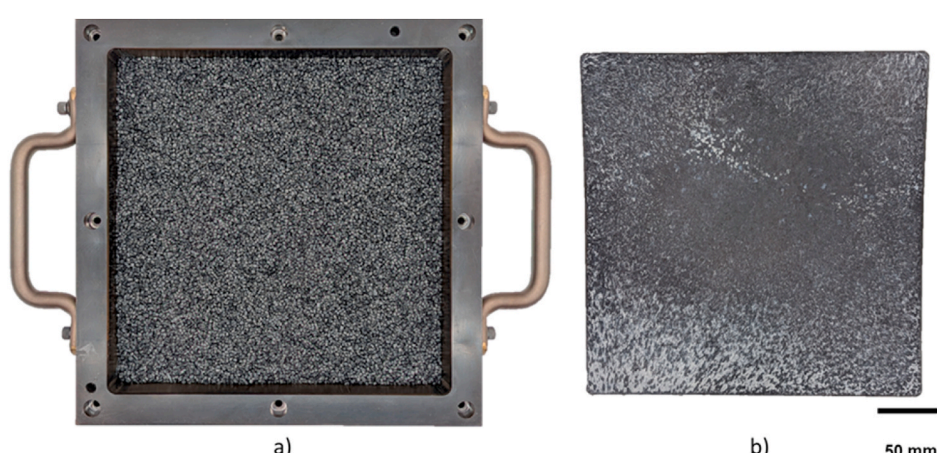


**Fig. 6.** (a) Virgin CF/PEEK pellets introduced in mould cavity and (b) Representative compression-moulded panel.

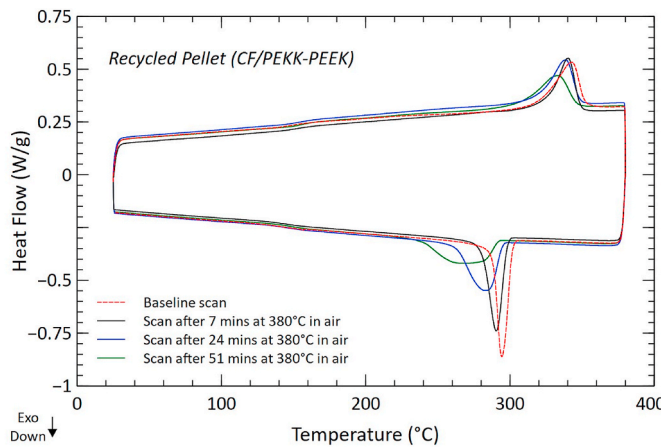


**Fig. 7.** DSC heating and cooling curves to characterize a recycled CF/PEKK-PEEK pellet after undergoing isothermal dwells of 7 min, 17 min and 27 min at 380 °C in air (see Fig. 3 and Table 1). The crystallization temperature and the degree of crystallization decrease with longer exposure to air, suggesting degradation of PEEK and PEKK.

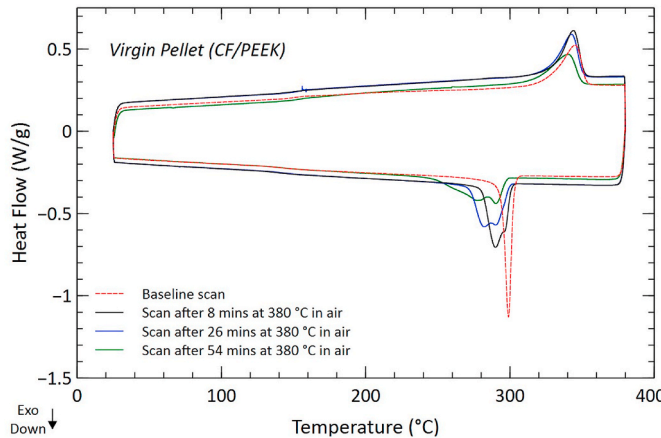


**Fig. 8.** DSC heating and cooling curves to characterize a virgin CF/PEEK pellet after undergoing isothermal dwells of 8 min, 18 min and 28 min at 380 °C in air (see Fig. 3 and Table 1). The degradation of PEEK is indicated by a reduced crystallization temperature.

suggesting the distinct crystalline structures are the result of reactions occurring during aging at 380 °C. However, these two peaks are not visible in the thermogram of the recycled pellets (Fig. 7). The matrix of the recycled pellets consists of a PEKK-PEEK blend, while the virgin pellets contain only PEEK. In PEKK-PEEK blends, the crystallization kinetics of PEEK may be hindered by the presence of PEKK, with PEEK crystallizing up to three times faster than PEKK [18].

Similar reasoning of Fig. 7 applies to Fig. 9, which shows the thermograms of the recycled CF/PEKK-PEEK pellets aged at the maximum temperature of 400 °C in air. The melting temperature shifted from 341 °C to 334 °C with a 41 % decrease in the melting enthalpy after the sample went through the whole aging cycle. Also, the shift in the crystallization temperature is more pronounced than for the specimen aged at 380 °C (Fig. 7). The shift in the crystallization temperature and the lower crystallinity and melting enthalpies point to a possible cross-linking reaction of the PEKK-PEEK polymer. Such a reaction is known to impede chain movement and reduce crystallinity.

The virgin specimen aged at 400 °C in air displays the same behaviour seen during aging at 380 °C (Fig. 8), with a reduction in both the enthalpy of fusion and the melting temperature, which decreases from 346 °C to 340 °C after the sample has gone through the entire aging cycle

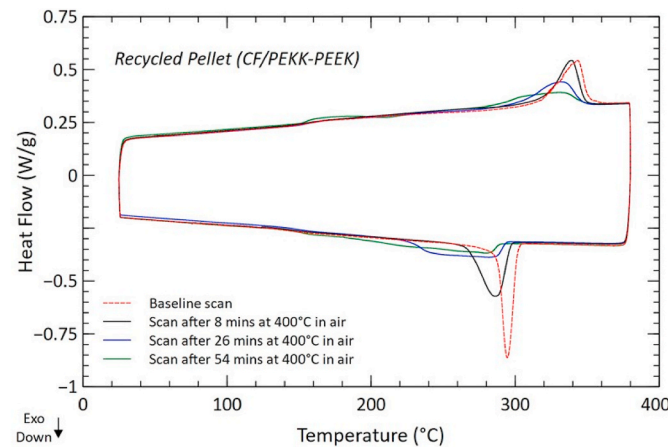


**Fig. 9.** DSC heating and cooling curves to characterize a recycled CF/PEKK-PEEK pellet after undergoing isothermal dwells of 8 min, 18 min and 28 min at 400 °C in air (see Fig. 3 and Table 1). The crystallization temperature and the degree of crystallization decrease with longer exposure to air, suggesting degradation of PEEK and PEKK.

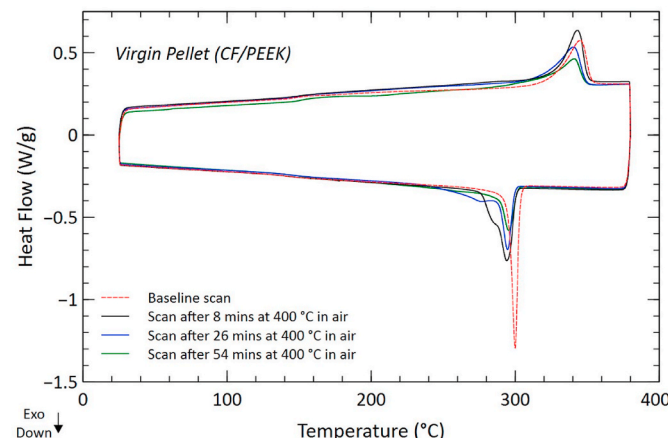


**Fig. 10.** DSC heating and cooling curves to characterize a virgin CF/PEEK pellet after undergoing isothermal dwells of 8 min, 18 min and 28 min at 400 °C in air (see Fig. 3 and Table 1). The degradation of PEEK is shown by the shift in the crystallization peak that becomes wider with longer exposure to air.

(Fig. 10). The presence of two distinct crystalline phases is shown again. However, the shift in the second crystallization peak is more evident than that observed for aging at 380 °C (Fig. 8). The progression of degradation is then indicated by the shift in the second crystallization peak, which becomes more pronounced after 26 min of aging and eventually absent after 54 min of aging.

The thermograms in Fig. 11 shows no shift in the melting temperature for the recycled CF/PEKK-PEEK samples aged at 380 °C and 400 °C in N<sub>2</sub>. This observation aligns with the results discussed by Day [9] in his study on PEEK filaments, demonstrating that the melting temperature shows minimal decrease even after exposure at 420 °C in N<sub>2</sub> for 2 h. As illustrated in Fig. 11, for specimens aged in N<sub>2</sub>, there is no shift in the crystallization temperature at 380 °C, while a slight decrease of 2 °C is observed for specimens heated to 400 °C. This is consistent with the oxidative nature of the crosslinking as seen in Figs. 7–10.

Recalling the potential degradation of PEEK and PEKK during the FGF process (see Section 2.3), additional DSC tests are performed on samples extracted from printed boxes. The samples extracted from the FGF boxes printed at 380 °C and 400 °C go through a single heating/cooling cycle to observe any changes in the crystallization peaks.

Fig. 12 presents the resulting thermograms and reveals no shift in the

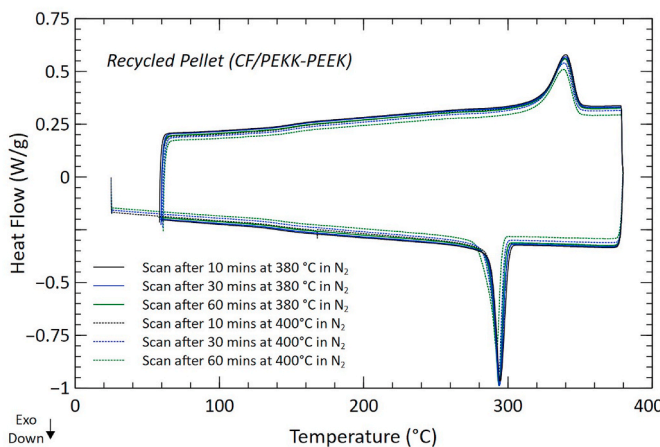


**Fig. 11.** DSC heating and cooling curves for a recycled pellet that underwent the cycle of Fig. 3 in  $N_2$ . No change in the crystallization peak is observed when pellets are aged in inert atmosphere.

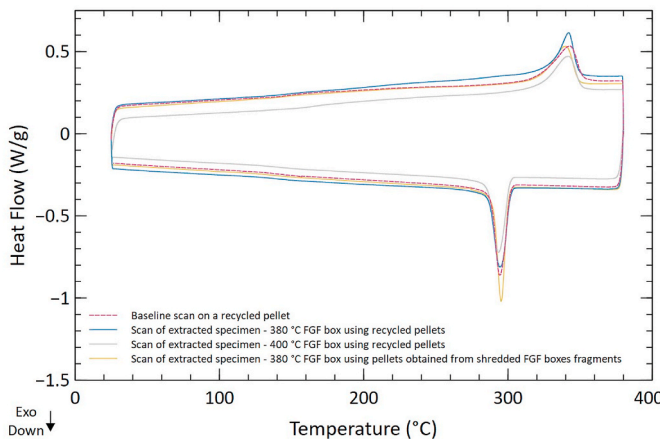


**Fig. 12.** DSC heat up and cool down curves for samples extracted from FGF boxes printed using recycled CF/PEKK-PEEK pellets or pellets obtained from shredded FGF box fragments at 380 °C or 400 °C. No sign of degradation can be observed.

crystallization temperature, indicating that degradation does not occur at either temperature during FGF processing. Notably, the polymer exposure durations to 380 °C and 400 °C in the extruder head are considerably shorter than the isothermal durations shown in Fig. 3 and Table 1. The results observed in Fig. 12 also suggest that the concentration of oxygen within the extruder head is insufficient to accelerate the crosslinking of PEEK and PEKK. Under the conditions mentioned, it can be assumed that the FGF is not influenced by the crosslinking degradation phenomenon previously noted.

### 3.2. Mechanical properties

This section presents the mechanical properties of the specimens extracted from FGF-manufactured boxes, highlighting their comparative performance against injection-moulded and compression-moulded parts produced from the same pellets. The FGF specimens are evaluated in two orientations – 0° and 90° relative to the filament extrusion direction – allowing to understand the anisotropic characteristics in strength and stiffness. Tensile and flexural test results are shown graphically in Figs. 13 and 14, respectively. Results for samples manufactured with virgin pellets are also included. For comparison, the data for injection moulding using virgin CF/PEEK pellets are taken from Syensqo datasheets.

The tensile modulus and strength of FGF specimens made with recycled CF/PEKK-PEEK pellets are significantly higher in the 0° direction compared to the 90° direction, showing increases of 283 % and 144 %, respectively. For specimens made using virgin CF/PEEK pellets, these increases are 258 % and 326 %. A similar behaviour is observed for flexural properties. The lower properties in the 90° direction are often attributed to improper bonding between filament layers during printing. For the current case in which the feedstock is made of fibre reinforced polymer, the alignment of fibre in the extrudate direction may also explain the better mechanical properties in the 0° direction.

In the 0° orientation, FGF specimens made with recycled CF/PEKK-PEEK pellets achieve tensile and flexural stiffness values of 78 % and 72 %, respectively, compared to injection-moulded specimens. The corresponding values for FGF specimens made using virgin CF/PEEK pellets are similar. A comparable behaviour is observed for the tensile and flexural strengths.

The results for compression-moulded specimens are also presented in Figs. 13 and 14. The compression-moulded panels exhibit significant warpage upon demoulding which is a common issue observed with ROS strand-based compression-moulded parts [19]. Tensile dogbones (Type I) and flexural coupons (12.7 × 127 mm rectangles) extracted from the panels are still deemed appropriate for testing due to the relaxation of

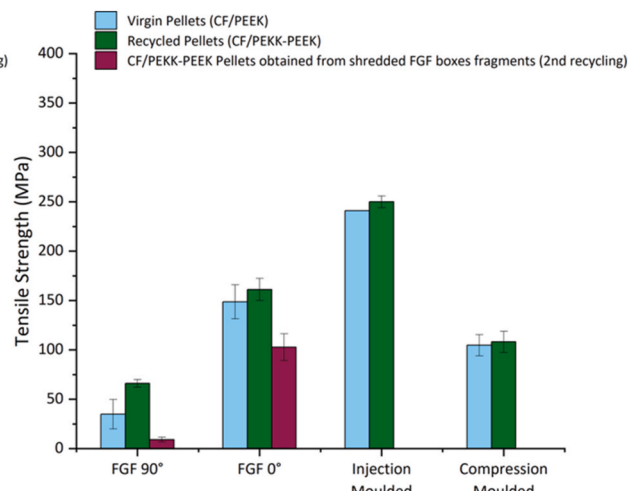
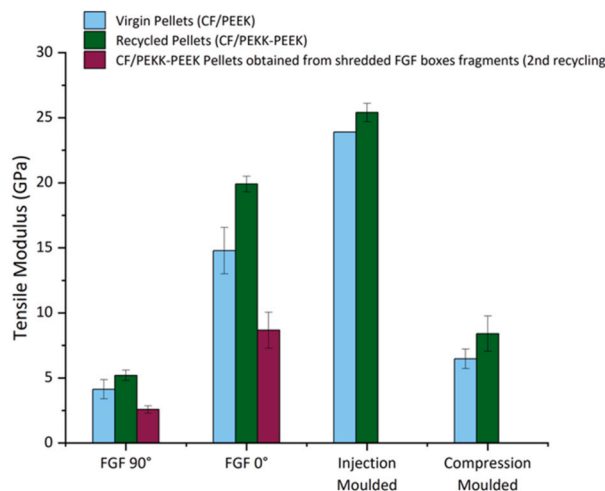


**Fig. 13.** Tensile properties of samples extracted from the FGF boxes or manufactured by injection moulding or compression moulding.

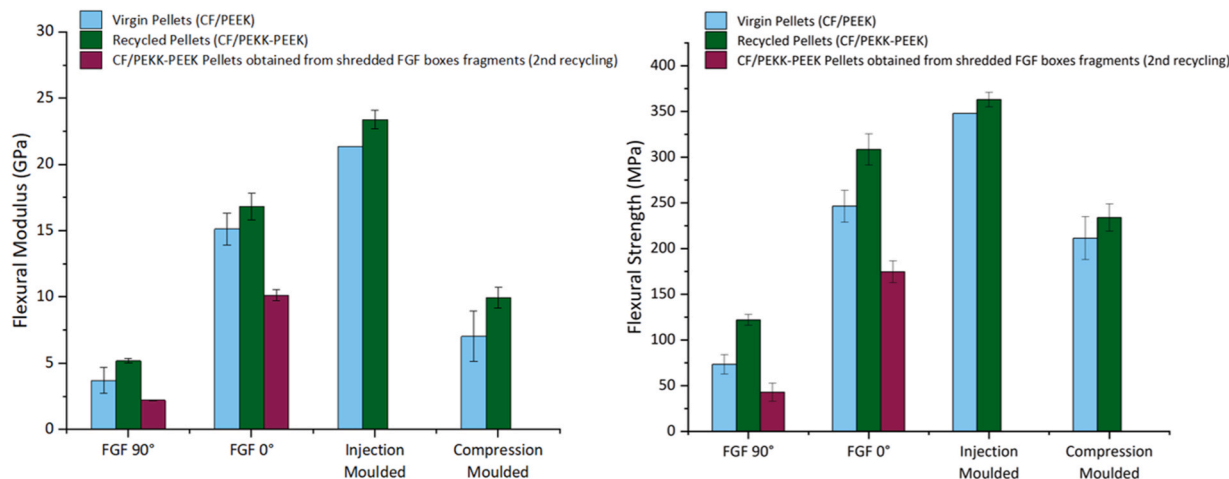


Fig. 14. Flexural properties of samples extracted from the FGF boxes or manufactured by injection moulding or compression moulding.

residual stresses during waterjet cutting. In terms of tensile stiffness and strength, the values of specimens made with recycled pellets reach 33 % and 43 % of those obtained in injection-moulded parts. The flexural values correspond to 43 % and 89 % of the injection-moulded parts, respectively. The samples made with virgin material follow the same trend. To the best of the authors' knowledge, the manufacturing of compression-moulded panels with pellets is not documented, leading to limited comparison. However, lower properties are expected for panels made with pellets instead of ROS strands, due to the shorter fibre length of pellets and the tendency for the pellets (and their fibres) to orient out-of-plane in the mould cavity, which contrasts with the typical in-plane orientation achieved by ROS strands. The available data for compression-moulded thermoplastic composite panels made with ROS

CF/PEEK strands notably includes panels with a fibre length varying from 5 to 50 mm [1]. It is also noted that the mechanical properties obtained here for the compression-moulded panels fall in between those of the FGF-0° and FGF-90° samples. This suggests that the mechanical performance is dictated by fibre orientation with the compression-moulded panels presenting randomly-oriented fibres while the FGF-90° and FGF-0° samples mostly consist of fibre perpendicular, and parallel, to the loading direction, respectively.

Fig. 15 illustrates the evolution of mechanical properties in relation to the FGF extrusion temperature (380 °C or 400 °C) and the specimen orientation (0° or 90°). The results indicate that stiffness and strength, in both tension and flexion, exhibit minimal variability with changes in extrusion temperature. Given the absence of degradation during the FGF

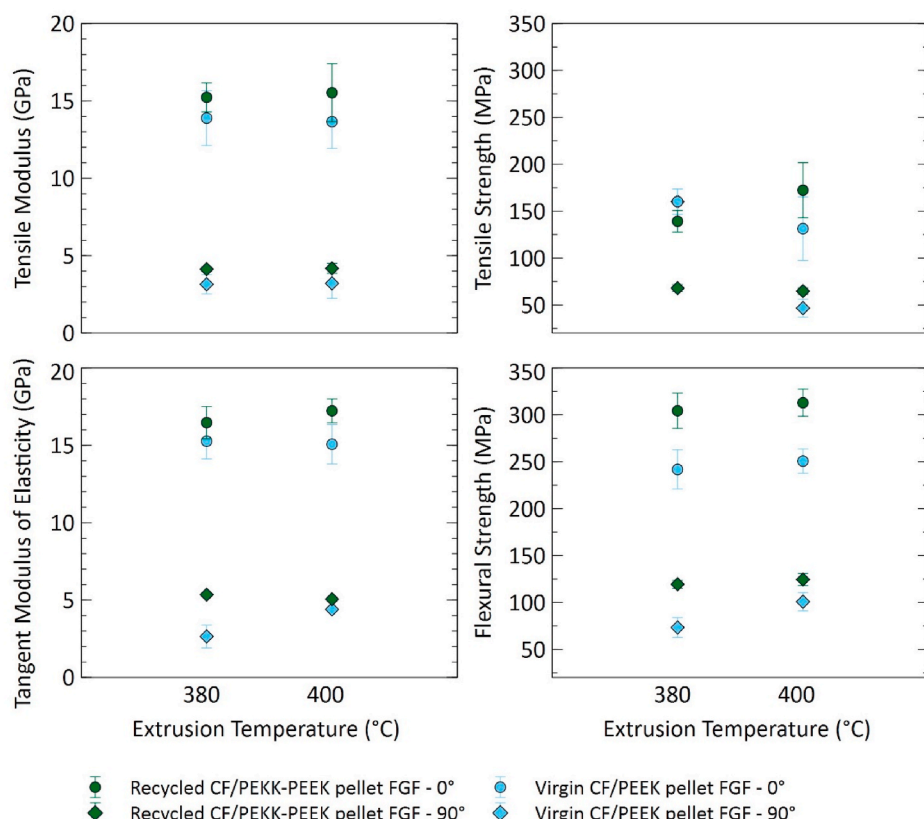


Fig. 15. Mechanical performance of samples extracted from the FGF boxes relative to extrusion temperature (Heat Zone 5).

process as previously discussed, these findings suggest that printing within the 380 °C–400 °C range does not significantly affect the mechanical properties. Future research should investigate how variations in viscosity might influence the ability to form parts with more complex geometries.

Table 7 summarizes the mechanical properties of FGF-manufactured specimens reported in the existing literature.

The tensile stiffness and strength values of FGF specimens made with recycled CF/PEKK-PEEK pellets are comparable to those of specimens made with virgin CF/PEEK material reported by Hu et al. [20]. This suggests that using recycled pellets is a promising alternative as a recycling route for manufacturing non-critical structural parts.

Figs. 13 and 14 also illustrate the properties of samples extracted from FGF boxes printed using twice-recycled pellets, i.e., obtained from shredded fragments (see Section 2.5). A comparison of the tensile and flexural results reveals that the second recycling cycle deteriorates the mechanical properties of the material, whether considering stiffness or strength and tensile or flexural properties. An explanation may reside in the shredding and pelletizing of the printed boxes causing polymer chain scission. As mentioned above, in order to investigate the effect of a second recycling, the printed boxes are shredded using an industrial shredder. The fragments are then shredded again using a smaller shredder to further reduce their size. And finally, the small fragments are pelletized. All these steps are likely to cause polymer chain scission. A lower polymer molecular weight due to chain scission may be directly responsible for lower stiffness and strength. In addition, chain scission may lead to a reduced polymer melt viscosity. In this work, the (once) recycled pellets were made from TET to which PEEK is added during pelletizing. They went through a manufacturing cycle very similar to the virgin pellets. Therefore, only the twice recycled pellets went through shredding steps and extra pelletizing, giving us confidence that the changed behaviour for the twice-recycled pellets comes from these manufacturing steps, that are likely to reduce the PEEK and PEKK molecular weight. This assumption of a lower melt viscosity is supported by visual observations made during the printing process. Fig. 16 shows an example of a FGF box printed using those twice-recycled pellets. Polymer flow altering the box geometry is visible, despite using the same printing parameters as for the virgin and the (once) recycled pellets. The flowing behaviour of the composite is clearly altered after two recycling cycles.

It is assumed that the shredding and pelletizing processes may also reduce the fibre length of the pellets, which may be a cause for lower mechanical properties of the twice-recycled pellets. Therefore, micro-CT is used to measure the fibre length in the recycled and twice-recycled CF/PEKK-PEEK pellets. As shown in Fig. 17, the fibre length decreases after the first industrial shredding and decreases again after the second

**Table 7**  
Summary of tensile properties for FGF specimens.

Author	Material	Extrusion Temperature (°C)	Nozzle Size (mm)	Tensile Stiffness (GPa)	Tensile Strength (MPa)
Present work	30 %wt. CF/PEKK-PEEK	380	9	19.9 <sup>a</sup>	161.2 <sup>a</sup>
Hu et al. [20]	20 %wt. CF/PEEK	390	3	16 <sup>b</sup>	180 <sup>b</sup>
	30 %wt. CF/PEEK	390	—	23.0	190.5
Philip [21]	PEEK 5600G	390	4	3.60	84.9
Tseng et al. [11]	PEEK 90G	390	0.3	3.83	94

<sup>a</sup> 0° orientation from Fig. 13.

<sup>b</sup> Approximation from graph in [20].

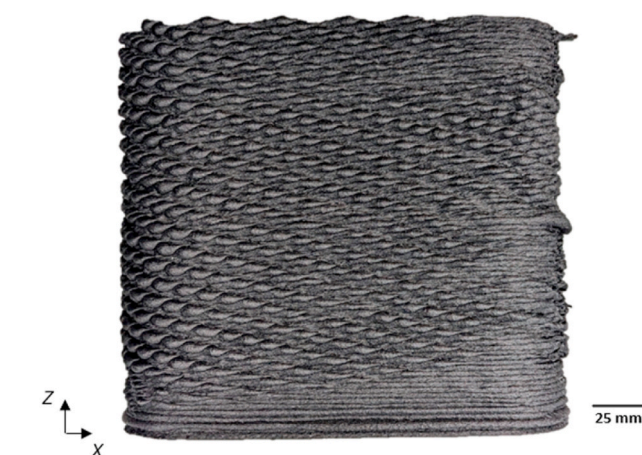


**Fig. 16.** FGF box printed using parameters of Table 2 with the twice-recycled pellets (pellets obtained from shredded printed boxes).

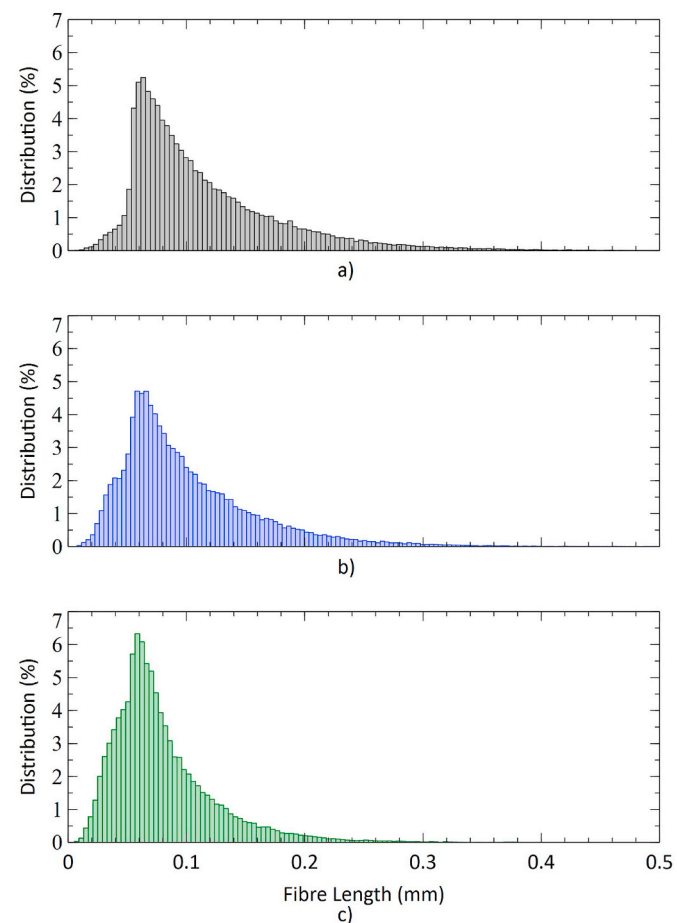


**Fig. 17.** Fibre length distribution of (a) Recycled CF/PEKK-PEEK pellets, (b) Recycled pellets after first shredding and (c) Recycled pellets after second shredding and pelletization.

shredding and pelletization.

Fig. 18 illustrates the cumulative fibre length distribution across shredding stages and after pelletization. It indicates that the second shredding and the pelletization (green curve) result in a larger proportion of shorter fibre compared to the fragments obtained from FGF boxes that are only shredded once (blue curve). The progressive shift of the curves suggests that repeated recycling leads to a reduction in average

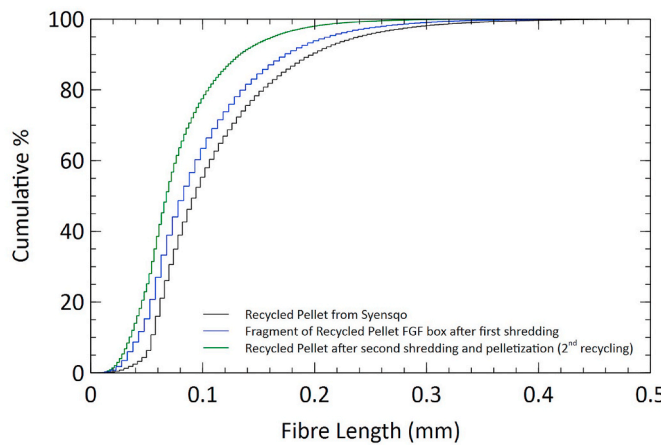


Fig. 18. Cumulative fibre length distribution across shredding stages.

fibre length. High shear forces within the extruder, either during the pelletization or the FGF process, are likely responsible for breaking fibres during the extrusion process, in addition to fibre being broken during shredding [22].

### 3.2.1. Microscopy

As stated above, the difference in the mechanical properties of the FGF-0° and FGF-90° samples is partly due to the carbon fibre of the composite being aligned in the filament direction during the extrusion process. This hypothesis is verified using SEM imaging. Fig. 19 illustrates the surfaces observed by microscopy in both 0° and 90° directions. Figs. 20 and 21 show representative fracture surface images of specimens made from recycled pellets. The same preferential fibre alignment was obtained on samples made from virgin pellets.

In particular, Fig. 20 shows the fracture surface of a 90° tensile sample from a box printed at 380 °C using the recycled CF/PEKK-PEEK pellets. Carbon fibres and imprints left by them are clearly visible on figure. A clear preferential fibre orientation (running horizontally on the figure) is visible. Such a preferential fibre orientation may explain, at least partially, the lower mechanical properties obtained with the 90°

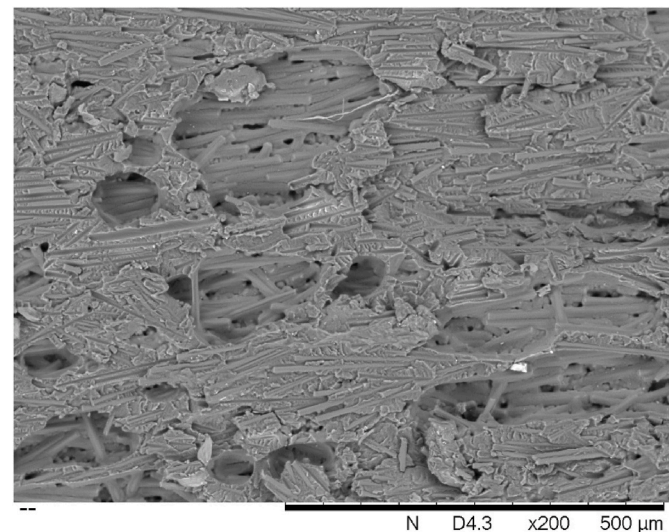


Fig. 20. SEM imaging of a fractured 90° tensile sample extracted from a box printed at 380 °C with recycled CF/PEKK-PEEK pellets. The fibres and fibre imprints can be seen running horizontally on the figure, showing clear preferential fibre alignment in the direction perpendicular to the loading direction.

samples. Another reason for the anisotropy may be incomplete healing of the interface between two adjacent filaments, which may be due to the printing parameters not being optimized.

Fig. 21 shows the fracture surface of a 0° sample. The fibres appear to have a consistent alignment in the same direction as the force applied during the tensile test, which corresponds to the extrusion direction.

## 4. Conclusions

This study demonstrates the feasibility of recycling thermoplastic composite TET waste into high-performance CF/PEKK-PEEK pellets suitable for use in the FGF process. By adding neat PEEK to the CF/PEKK TET waste, the resulting pellets exhibit good printability, making them viable feedstock for large-scale additive manufacturing.

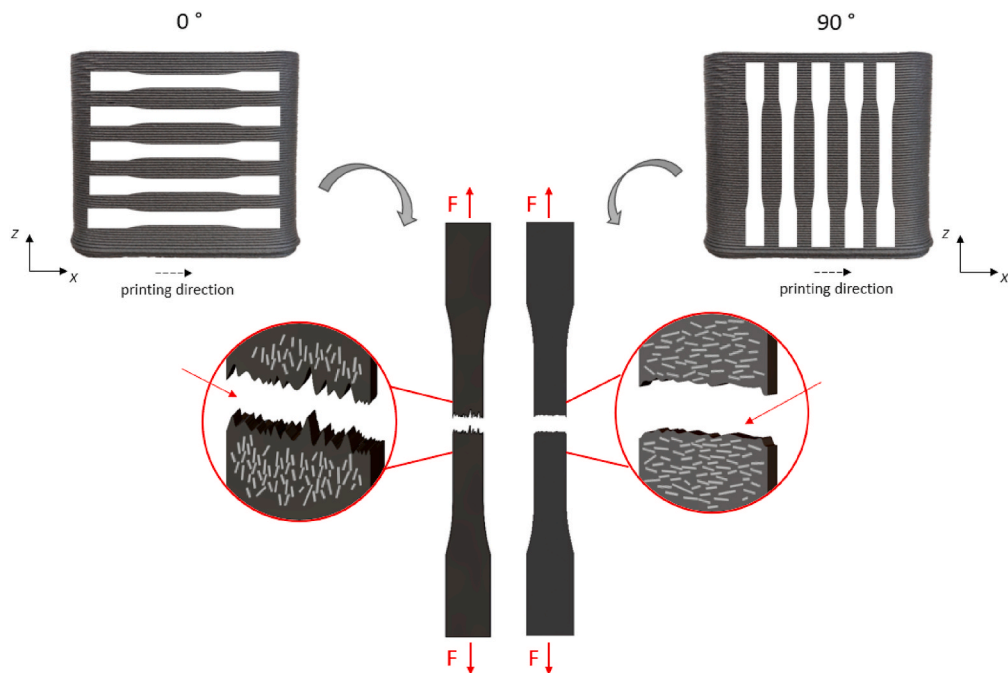
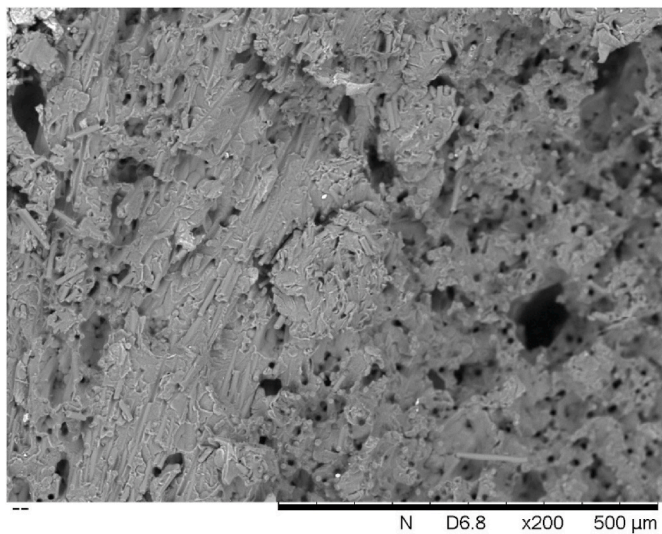


Fig. 19. Schematic of the tensile 0° and 90° fracture surfaces observed by SEM.



**Fig. 21.** SEM imaging of a fractured 0° sample under tensile loading extracted from a box printed at 380 °C with recycled CF/PEKK-PEEK pellets. The holes seen on the sample surface show that fibres run perpendicular to the figure plane.

Thermal analysis revealed that, while oxidative degradation of PEEK and PEKK occurs during long exposure to typical processing temperature conditions, no significant degradation is observed in specimens manufactured via FGF. The mechanical properties of parts printed from recycled pellets showed anisotropy typical of extrusion-based processes, with stiffness and strength reduction for the samples tested perpendicular to the filament direction. A second recycling cycle led to a notable reduction in material performance, attributed to chain scission and reduction in fibre length after shredding and pelletization.

Thermoplastic composite pre-impregnated production waste (TET) can be recycled by the compression moulding process, without any prior transformation. The TET then act as ROS and can achieve various complex geometries thanks to their excellent processability. Here, it is shown that the FGF process, although requiring prior transformation of the TET into printable pellets, offers a sustainable and practical approach to repurposing manufacturing waste. This process offers enhanced manufacturing flexibility and is particularly suitable for applications such as rapid prototyping and mould fabrication. Future work should identify methods to mitigate degradation during multiple recycling cycles and explore potential applications for a material with reduced mechanical properties and altered physical properties.

#### CRediT authorship contribution statement

**Ruan-Isabelle Richard Soucy:** Writing – original draft, Investigation, Formal analysis, Data curation. **Adam W. Smith:** Writing – review & editing, Methodology, Investigation, Formal analysis. **Kevin Dupuis:** Writing – review & editing, Resources. **Ilyass Tabiai:** Writing – review & editing, Supervision. **Martine Dubé:** Writing – review & editing, Supervision, Methodology, Funding acquisition, Conceptualization.

#### Declaration of competing interest

The authors declare that they have no known competing financial interests or personal relationships that could have appeared to influence the work reported in this paper.

#### Acknowledgements

The authors would like to thank Joël Grignon, Anthony Remington and Serge Plamondon for their technical assistance. This study was made

possible with the financial support provided by the Marcelle Gauvreau Research Chair on Sustainable Composite Materials, CREPEC, MITACS (IT35457) and Syensqo (previously part of Solvay group).

#### Data availability

Data will be made available on request.

#### References

- [1] H. Pattery, A.W. Smith, A. Pik, J.-P. Canart, I. Tabiai, M. Dubé, Characterisation of defects in strands-based thermoplastic composite parts using ultrasonic inspection, in: SAMPE Conference, May 20-23, 2024, Long Beach, CA, USA.
- [2] H. Pattery, A.W. Smith, J.-P. Canart, I. Tabiai, M. Dubé, Mechanical sieving of Carbon-Fibre/PEEK prepreg tape edge trim waste prior to compression moulding and its influence on panel properties, in: International Conference on Composite Materials, July 30th – August 4th, 2023, Belfast, United Kingdom.
- [3] J. Avenet, Assemblage Par Fusion De Composites À Matrice Thermoplastique : Caractérisation Expérimentale Et Modélisation De La Cinétique d'auto-adhésion Hors Équilibre, Université de Nantes (UN), 2021. Thèse de doctorat, <https://theses.hal.science/tel-03405352>.
- [4] E. Courvoisier, Y. Bicaba, X. Colin, Analyse de la dégradation thermique du Poly (éther éther cétones), Matériaux Tech. 105 (4) (2017) 403, <https://doi.org/10.1051/matech/2018007>.
- [5] A. Benarbia, V. Sobotka, N. Boyard, C. Roua, Modelling the melting kinetics of polyetheretherketone depending on thermal history: application to additive manufacturing, <https://doi.org/10.3390/polym16101319>, 2024.
- [6] T. Choupin, Mechanical performances of PEKK thermoplastic composites linked to their processing parameters, ENSAM, Paris, ParisTech (2017).
- [7] T. Choupin, B. Fayolle, G. Régnier, C. Paris, J. Cinquin, B. Brûlé, Macromolecular modifications of Poly(Etherketoneketone) (PEKK) copolymer at the melting state, Polym. Degrad. Stabil. 155 (2018) 103–110, <https://doi.org/10.1016/j.polymdegradstab.2018.07.005>.
- [8] M. Day, D. Sally, D.M. Wiles, Thermal degradation of Poly(Aryl-Ether-Ether-Ketone): experimental evaluation of crosslinking reactions, J. Appl. Polym. Sci. 40 (9–10) (1990) 1615–1625, <https://doi.org/10.1002/app.1990.070400917>.
- [9] M. Day, T. Suprunchuk, J.D. Cooney, D.M. Wiles, Thermal degradation of Poly (Aryl-Ether-Ether-Ketone) (PEEK): a differential scanning calorimetry study, J. Appl. Polym. Sci. 36 (5) (1988) 1097–1106, <https://doi.org/10.1002/app.1988.070360510>.
- [10] O. De Almeida, L. Feuillerat, J.-C. Fontanier, F. Schmidt, Determination of a degradation-induced limit for the consolidation of CF/PEEK composites using a thermo-kinetic viscosity model, Compos. Appl. Sci. Manuf. 158 (2022) 106943, <https://doi.org/10.1016/j.compositesa.2022.106943>.
- [11] J.-W. Tseng, C.-Y. Liu, Y.-K. Yen, J. Belkner, T. Bremicker, B.H. Liu, T.-J. Sun, A.-B. Wang, Screw extrusion-based additive manufacturing of PEEK, Mater. Des. 140 (2018) 209–221, <https://doi.org/10.1016/j.matdes.2017.11.032>.
- [12] A. Curni, A. Rochman, J. Buhagiar, Influence of polyether ether ketone (PEEK) viscosity on interlayer shear strength in screw extrusion additive manufacturing, Addit. Manuf. 84 (2024) 104086, <https://doi.org/10.1016/j.addma.2024.104086>.
- [13] P. Wang, B. Zou, S. Ding, L. Li, C. Huang, Effects of FDM-3D printing parameters on mechanical properties and microstructure of CF/PEEK and GF/PEEK, Chin. J. Aeronaut. 34 (9) (2021) 236–246, <https://doi.org/10.1016/j.cja.2020.05.040>.
- [14] CEAD Large Scale, Additive manufacturing E25 brochure. <https://ceadgroup.com/solutions/technology-components/e25/>.
- [15] S. Kandurthi, F. Tran, S. Chen, J. Mapkar, M. Haq, Bead geometry-induced stress concentration factors in material extrusion polymer additive manufacturing, Rapid Prototyp. J. 29 (7) (2023) 1438–1452, <https://doi.org/10.1108/RPJ-11-2022-0404>.
- [16] A. Mortier, Étude des propriétés de moules recyclés réalisés par fabrication additive grand format, Rapport de projet, École de technologie supérieure (2022) 94.
- [17] H. Zhang, Fire-Safe Polymers and Polymer Composites, University of Massachusetts, 2003. PhD Thesis, <https://www.proquest.com/docview/305322385/abstract/A477495820A04E77PQ/1>.
- [18] Wu Wang, Jerold M. Schultz, Benjamin S. Hsiao, Dynamic study of Crystallization- and melting-induced phase separation in PEEK/PEKK blends, Macromolecules 30 (16) (1997) 4544–4550, <https://doi.org/10.1021/ma9700921>.
- [19] C. Collins, Dimensional Stability in compression-moulded Discontinuous Long Fibre carbon/PEEK Composites, McGill University, 2018. PhD Thesis, <https://escholarship.mcgill.ca/concern/theses/vq27zq96g>.
- [20] Z. Hu, J. He, W. Chen, W. Liu, J. Ding, C. He, S. Wang, F. Ning, X. Li, High-performance carbon fiber reinforced polyether-ether-ketone composite pellets 3D-Printed via screw-extrusion additive manufacturing, Compos. Sci. Technol. 246 (2024) 110362, <https://doi.org/10.1016/j.compscitech.2023.110362>.
- [21] A.A. Philip, Development of a large-scale continuous carbon fiber composite additive manufacturing system based on fused granular fabrication. <https://doi.org/10.7939/r3-92ev-r111>, 2024.
- [22] M. Korey, M.L. Rencheck, H. Tekinalp, S. Wasti, P. Wang, S. Bhagia, R. Walker, T. Smith, X. Zhao, M.E. Lamm, K. Copenhagen, U. Vaidya, S. Ozcan, Recycling polymer composite granulate/regrind using big area additive manufacturing, Compos. B Eng. 256 (2023) 110652, <https://doi.org/10.1016/j.compositesb.2023.110652>.